UNIVERSITY OF WEST BOHEMIA

Applied and Computational Mechanics 3 (2009) 63–74

Applied and Computational Mechanics

Contribution to the gas flow and heat transfer modelling in microchannels

H. Klášterka[a,*], J. Vimmr[b], M. Hajžman[b]

[a] *Faculty of Mechanical Engineering, University of West Bohemia, Univerzitní 22, 306 14 Pilsen, Czech Republic*
[b] *Faculty of Applied Sciences, University of West Bohemia, Univerzitní 22, 306 14 Pilsen, Czech Republic*

Received 26 January 2009; received in revised form 6 May 2009

Abstract

This study is focused on the mathematical modelling of gas flow and heat transfer in a microchannel with the rectangular cross-section. The gas flow is considered to be steady, laminar, incompressible, hydrodynamically and thermally fully developed. The main objective is the application of the slip flow boundary conditions — the velocity slip and the temperature jump at microchannel walls. The analytical solution of both flow and heat transfer is derived using the Fourier method and it is also compared with the numerical solution based on the finite difference method applied on the Poisson's equations describing gas flow and heat transfer in the microchannel.

Keywords: rectangular microchannel, slip flow regime, heat transfer, analytical solution, numerical solution

1. Introduction

The interest in the study of fluid flow and heat transfer in microchannels has been increasing a lot in the last few decades. Microflows are not only typical for biological systems (capillaries, brain, lungs, kidneys etc.) but also for many man-made technical systems such as heat exchangers, nuclear reactors or microturbines. In such objects, very small characteristic dimensions of microchannels and microtubes result in flows with very low Reynolds numbers. If the characteristic dimensions are comparable to the mean free path of the molecules, the microflow does not behave like a continuum and the molecular structure of the fluid has a significant influence on the microflow character. The ratio $Kn = \lambda/D_h = Ma/Re\sqrt{\pi\gamma/2}$ is the Knudsen number, which can be related to the Reynolds and Mach numbers [6], and it plays a very important role in gas microflows. Here, λ is the molecular mean free path, D_h is the hydraulic diameter of the microchannel and γ is the specific heat ratio.

According to the value of the Knudsen number, the gas flow and heat transfer can be divided into the following flow regimes, [6] or [7]: the continuum flow regime for $Kn < 10^{-3}$; the slip flow regime for $10^{-3} < Kn < 10^{-1}$ (the Navier-Stokes equations remain applicable, a velocity slip and a temperature jump are taken into account at the channel walls); the transition flow regime for $10^{-1} < Kn < 10$ (the continuum approach of the Navier-Stokes equations is no longer valid, but intermolecular collisions should be taken into account) and the free molecular flow regime for $Kn > 10$ (the occurance of intermolecular collisions is negligible compared with collisions between the gas molecules and the microchannel wall). It is known that characteristic dimensions of the channel, which do not have to be micrometric, and low

*Corresponding author. Tel.: +420 377 638 139, e-mail: klast@kke.zcu.cz.

values of pressure can lead to high Knudsen numbers. However, the same situation can occur for atmospheric pressure, when the characteristic dimensions of the channel are nanometric. Theoretically, the Navier-Stokes equations are the first-order approximation of the Chapman-Enskog solution for the Bolzmann equation and they are also first-order accurate in Kn.

The classical continuum flow regime may be accurately modelled by the system of the full Navier-Stokes equations completed by the equation of state and classical non-slip boundary conditions $\boldsymbol{u}|_w = \boldsymbol{u}_{wall}$, $T|_w = T_{wall}$, that express the continuity of the velocity and the temperature between the fluid and the channel wall. In the close vicinity of the wall, the so-called Knudsen layer occurs in which the gas is out of thermodynamic equilibrium. This layer has a thickness comparable with the mean free path of molecules. For very low Knudsen numbers (in the continuum flow regime), the effect of the Knudsen layer is negligible. However, in the slip flow regime, the influence of the Knudsen layer must be taken into account providing the classical non-slip boundary conditions are modified so that they express the velocity slip and the temperature jump at channel walls. From [8] it is known that Kundt and Wartburg in 1875 and Maxwell in 1879 were probably the first who mentioned the velocity slip and the temperature jump at the wall. For a gas flow in the direction s parallel to the wall, the first-order velocity slip and temperature jump boundary conditions have taken the form, [6],

$$u_{slip} = u_s - u_{wall} = \frac{2-\sigma}{\sigma}\lambda\frac{\partial u_s}{\partial n}\Big|_w + \frac{3}{4}\frac{\eta}{\rho T}\frac{\partial T}{\partial s}\Big|_w, \tag{1}$$

$$T - T_{wall} = \frac{2-\sigma_T}{\sigma_T}\frac{2\gamma}{\gamma+1}\frac{k}{\eta c_v}\lambda\frac{\partial T}{\partial n}\Big|_w. \tag{2}$$

Here the dimensionless coefficient σ is the tangential momentum accommodation coefficient and the dimensionless coefficient σ_T is the energy accommodation coefficient. The overview of higher-order slip flow boundary conditions is presented for example in [6] or [7]. However, many authors use the first-order slip flow boundary conditions (1)–(2) with neglected second term in (1).

From the theoretical point of view, the slip flow regime is particularly interesting because it generally leads to analytical or semi-analytical models which allow us to calculate velocities, flow rates and temperature fields for fully developed laminar microflows. For example, in [2], the problem of compressibility of gas flow between two parallel plates is studied analytically. Numerical solution of the same problem is given in [1]. Analytical solution of three-dimensional fully developed laminar slip flow in rectangular microchannels is given in [3, 10]. Analytical determination of temperature field and Nusselt number between two parallel plates, including axial heat transfer, temperature jump and viscous dissipation, is studied in paper [5]. The works [11, 9] are devoted to the analytical solution of temperature field and Nusselt number computation in three-dimensional rectangular microchannels. The flow is supposed to be steady, laminar, incompressible, fully hydrodynamically and thermally developed. Let us note, that further examples of laminar flow and heat transfer in various microchannels and microtubes are given in [6].

The main objective of this study is the comparison of our analytical and numerical solution of the gas flow and heat transfer in a 3D microchannel with rectangular cross-section in the slip flow regime. The gas flow is assumed to be laminar, incompressible, steady, hydrodynamically and thermally fully developed applying the first-order velocity slip and temperature jump boundary conditions. The Fourier method is used for our analytical solution, resulting in expressions that seem to be simpler to evaluate than the analytical solution presented in [10]. The good agreement with numerical results also proves the correctness of our analytical formulation.

2. Mathematical formulation of the problem

Let us consider a steady laminar flow of an incompressible fluid in a long microchannel with a rectangular cross-section. The microchannel dimensions are illustrated in fig. 1, where $L = 5 \cdot 10^{-3}$ m is the microchannel length and the rectangle sides are considered as $2h = 10^{-6}$ m and $2b = 2 \cdot 10^{-5}$ m.

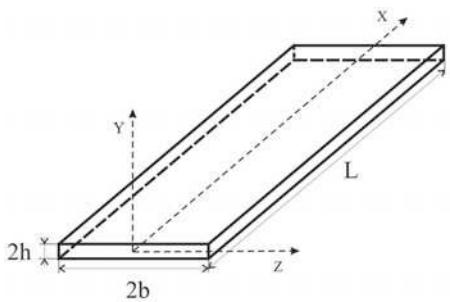

Fig. 1. Geometry of the microchannel with the rectangular cross-section

Velocity field

The incompressible gas flow can be described by the non-linear system of the Navier-Stokes equations, [4]. Because we suppose the fully developed flow, we can assume $\partial u/\partial x = 0$. Furthermore, the cross-sectional components v, w of the velocity vector can be considered as very small compared to the longitudinal velocity u. Thus, the non-linear system of the Navier-Stokes equations reduces to

$$\frac{\partial^2 u}{\partial y^2} + \frac{\partial^2 u}{\partial z^2} = \frac{1}{\eta}\frac{\mathrm{d}p}{\mathrm{d}x}, \tag{3}$$

$$\frac{\partial p}{\partial y} = \frac{\partial p}{\partial z} = 0, \tag{4}$$

which means that $p = p(x)$ and $u = u(y, z)$. Since the microchannel is symmetrical with respect to the planes xz and xy, we can write the boundary conditions

$$\left(\frac{\partial u}{\partial y}\right)_{y=0} = 0, \quad \left(\frac{\partial u}{\partial z}\right)_{z=0} = 0. \tag{5}$$

As mentioned before, we assume the slip flow boundary conditions at the microchannel walls. In our work, we neglect the second right-hand side term in (1) and use $\sigma = 1$, $\sigma_T = 1$ in (1), (2), respectivelly. Then we can write

$$u(\pm h, z) = -KnD_h \left(\frac{\partial u}{\partial y}\right)_{y=\pm h}, \quad u(y, \pm b) = -KnD_h \left(\frac{\partial u}{\partial z}\right)_{z=\pm b}, \tag{6}$$

where D_h is the hydraulic diameter

$$D_h = \frac{4bh}{b+h}. \tag{7}$$

Temperature field

The temperature distribution in case of the steady, laminar and incompressible flow in the long microchannel with the rectangular cross-section can be described by the equation

$$U_{avg}\frac{\partial T}{\partial x} = a\left(\frac{\partial^2 T}{\partial y^2} + \frac{\partial^2 T}{\partial z^2}\right), \tag{8}$$

where $a = \frac{k}{c_p\rho}$ is the thermal conductivity coefficient (c_p is the specific heat for constant pressure, k is the heat conductivity). The average velocity U_{avg} is defined as

$$U_{avg} = \frac{1}{bh}\int_0^h \int_0^b u(y,z)\,\mathrm{d}z\,\mathrm{d}y. \tag{9}$$

Further, we will also operate with the average temperature which is defined similarly

$$T_{avg} = \frac{1}{bh}\int_0^h \int_0^b T(y,z)\,\mathrm{d}z\,\mathrm{d}y. \tag{10}$$

From the heat balance we know

$$c_p\rho U_{avg}\frac{\partial T}{\partial x}4bh\,\mathrm{d}x = (4b\,\mathrm{d}x + 4h\,\mathrm{d}x)q, \tag{11}$$

that is

$$U_{avg}\frac{\partial T}{\partial x} = \frac{q}{c_p\rho}\frac{b+h}{bh} = Qa, \tag{12}$$

where q is the heat flux and Q is defined by (12). Using (8) we can finally write

$$\frac{\partial^2 T}{\partial y^2} + \frac{\partial^2 T}{\partial z^2} = Q. \tag{13}$$

The symmetry boundary conditions are expressed as

$$\left(\frac{\partial T}{\partial y}\right)_{y=0} = 0, \quad \left(\frac{\partial T}{\partial z}\right)_{z=0} = 0 \tag{14}$$

and the temperature jump at the walls is described by the relations

$$T_w - T(\pm h, z) = \frac{2\gamma}{\gamma+1}KnD_h\frac{1}{Pr}\left(\frac{\partial T}{\partial y}\right)_{y=\pm h}, \tag{15}$$

$$T_w - T(y, \pm b) = \frac{2\gamma}{\gamma+1}KnD_h\frac{1}{Pr}\left(\frac{\partial T}{\partial z}\right)_{z=\pm b}, \tag{16}$$

where Pr is the Prandtl number.

Dimensionless model

Relating the coordinates x, y, z to D_h, the velocity u to the average velocity U_{avg}, the temperature T to the average temperature T_{avg} and the static pressure p to the reference pressure

$p_{ref} = \rho U_{avg}^2$, we obtain the dimensionless form of the problem. From now, we will consider all the quantities as dimensionless. The equation (3) now has the dimensionless form

$$\frac{\partial^2 u}{\partial y^2} + \frac{\partial^2 u}{\partial z^2} = Re \frac{\mathrm{d}p}{\mathrm{d}x}, \tag{17}$$

the dimensionless form of the velocity slip boundary conditions (6) is

$$u(\pm h, z) = -Kn \left(\frac{\partial u}{\partial y} \right)_{y=\pm h}, \quad u(y, \pm b) = -Kn \left(\frac{\partial u}{\partial z} \right)_{z=\pm b} \tag{18}$$

and the boundary conditions expressing the symmetry remain unchanged, so the equations (5) still hold for dimensionless quantities. In the equation (17), we consider the Reynolds number as $Re = U_{avg} \rho D_h / \eta$.

Regarding the temperature field, the dimensionless form of the equation (8) can be written as

$$\frac{\partial T}{\partial x} = \frac{a}{U_{avg} D_h} \left(\frac{\partial^2 T}{\partial y^2} + \frac{\partial^2 T}{\partial z^2} \right) \equiv \frac{1}{Pe} \left(\frac{\partial^2 T}{\partial y^2} + \frac{\partial^2 T}{\partial z^2} \right), \tag{19}$$

where $Pe = Re \cdot Pr$ is the Peclet number. The symmetry conditions (14) do not change for dimensionless quantities and the temperature jump boundary conditions are now

$$T_w - T(\pm h, z) = \frac{2\gamma}{\gamma + 1} \frac{Kn}{Pr} \left(\frac{\partial T}{\partial y} \right)_{y=\pm h}, \quad T_w - T(y, \pm b) = \frac{2\gamma}{\gamma + 1} \frac{Kn}{Pr} \left(\frac{\partial T}{\partial z} \right)_{z=\pm b}. \tag{20}$$

3. Analytical and numerical solution of incompressible fluid flow

With regard to the mentioned planes of symmetry, let us firstly focus on the analytical solution of the flow problem described by the equation (17) with dimensionless boundary conditions (5) and (18) in the domain given by $y \in \langle 0; h \rangle$, $z \in \rangle 0; b \langle$. We expect the solution in the form

$$u(y, z) = u^{(1)}(z) + u^{(2)}(y, z). \tag{21}$$

and after substituting (21) into (17) we get two differential equations

$$\frac{\mathrm{d}^2 u^{(1)}(z)}{\mathrm{d}z^2} = Re \frac{\mathrm{d}p}{\mathrm{d}x}, \tag{22}$$

$$\frac{\partial^2 u^2(y, z)}{\partial y^2} + \frac{\partial^2 u^{(2)}(y, z)}{\partial z^2} = 0. \tag{23}$$

We can express the general solution of equation (22) as

$$u^{(1)}(z) = \frac{Re}{2} \frac{\mathrm{d}p}{\mathrm{d}x} z^2 + C_1 z + C_2 \tag{24}$$

and the solution of the equation (23) is expected to be a product of two functions $f(y)$ and $g(z)$

$$u^{(2)}(y, z) = f(y) g(z). \tag{25}$$

Substituting (25) into (23) we get

$$\frac{1}{f(y)} \frac{\mathrm{d}^2 f(y)}{\mathrm{d}y^2} = -\frac{1}{g(z)} \frac{\mathrm{d}^2 g(z)}{\mathrm{d}z^2} = \kappa^2, \tag{26}$$

where κ is the unknown constant. Thus, the treatment of the partial differential equation (23) is transformed to the solution of two ordinary differential equations

$$\frac{\mathrm{d}^2 f(y)}{\mathrm{d}y^2} - \kappa^2 f(y) = 0, \quad \frac{\mathrm{d}^2 g(z)}{\mathrm{d}z^2} + \kappa^2 g(z) = 0 \tag{27}$$

generally having the solution

$$f(y) = A_1 e^{\kappa y} + A_2 e^{-\kappa y} \quad \text{and} \quad g(z) = B_1 \cos(\kappa z) + B_2 \sin(\kappa z), \tag{28}$$

and therefore according to (25) we get

$$u^{(2)}(y,z) = \left(A_1 e^{\kappa y} + A_2 e^{-\kappa y}\right) \left[B_1 \cos(\kappa z) + B_2 \sin(\kappa z)\right]. \tag{29}$$

Now, we can rewrite the solution (21) as

$$u(y,z) = \frac{Re}{2}\frac{\mathrm{d}p}{\mathrm{d}x} z^2 + C_1 z + C_2 + \left(A_1 e^{\kappa y} + A_2 e^{-\kappa y}\right) \left[B_1 \cos(\kappa z) + B_2 \sin(\kappa z)\right], \tag{30}$$

which must satisfy the boundary conditions (5) and (18). The symmetry conditions (5) yield

$$C_1 = 0, \quad A_1 = A_2, \quad B_2 = 0. \tag{31}$$

Afterwards, the solution (30) reduces to

$$u(y,z) = \frac{Re}{2}\frac{\mathrm{d}p}{\mathrm{d}x} z^2 + C_2 + A \cosh(\kappa y) \cos(\kappa z), \tag{32}$$

where $A = 2A_1B_1$. To derive the remaining constants A, C_2, κ we will use the boundary conditions (18), so we get

$$\frac{Re}{2}\frac{\mathrm{d}p}{\mathrm{d}x} z^2 + C_2 + A \cosh(\kappa h) \cos(\kappa z) = -\kappa Kn A \sinh(\kappa h) \cos(\kappa z), \tag{33}$$

$$\frac{Re}{2}\frac{\mathrm{d}p}{\mathrm{d}x} b^2 + C_2 + A \cosh(\kappa y) \cos(\kappa b) = -Kn \left[Re \frac{\mathrm{d}p}{\mathrm{d}x} b - A\kappa \cosh(\kappa y) \sin(\kappa b)\right]. \tag{34}$$

In order to be the equation (34) fulfilled for every $y \in \langle 0; h \rangle$, following conditions have to be satisfied

$$C_2 = -\frac{Re}{2}\frac{\mathrm{d}p}{\mathrm{d}x} b^2 \left(1 + \frac{2Kn}{b}\right), \tag{35}$$

$$\frac{\cot(\kappa b)}{\kappa b} = \frac{Kn}{b}. \tag{36}$$

The transcendent equation (36) has an infinite number of roots $\kappa b = \kappa_i b$, $i = 1, \ldots, \infty$, and therefore we can write the solution (32) as

$$u(y,z) = \frac{Re}{2}\frac{\mathrm{d}p}{\mathrm{d}x} \left[z^2 - b^2 \left(1 + \frac{2Kn}{b}\right)\right] + \sum_{i=1}^{\infty} A_i \cosh(\kappa_i y) \cos(\kappa_i z). \tag{37}$$

The last step is to determine the constants A_i using (33) and (35) that result in

$$\sum_{i=1}^{\infty} A_i \left[\cosh(\kappa_i h) + \kappa Kn A \sinh(\kappa_i h)\right] \cos(\kappa_i z) = \frac{Re}{2}\frac{\mathrm{d}p}{\mathrm{d}x} b^2 \left(1 + \frac{2Kn}{b} - \frac{z^2}{b^2}\right). \tag{38}$$

Multiplying this equation by $\cos(\kappa_j z)\,\mathrm{d}z$, where j is any given value of i, and integrating over the interval $\langle 0; b\rangle$, we get

$$A_i = \frac{Re\frac{\mathrm{d}p}{\mathrm{d}x}\frac{b}{\kappa_i^2}\left[-\cos(\kappa_i b) + \left(Kn\kappa_i + \frac{1}{\kappa_i b}\right)\sin(\kappa_i b)\right]}{\left[\cosh(\kappa_i h) + Kn\kappa_i \sinh(\kappa_i h)\right]\left[\frac{b}{2} + \frac{\sin(2\kappa_i b)}{4\kappa_i}\right]} \tag{39}$$

and finally we can write the solution as

$$\begin{aligned} u(y,z) &= \frac{Re}{2}\frac{\mathrm{d}p}{\mathrm{d}x}\left[z^2 - b^2\left(1 + \frac{2Kn}{b}\right)\right] + \\ &+ \sum_{i=1}^{\infty} \frac{Re\frac{\mathrm{d}p}{\mathrm{d}x}\frac{b}{\kappa_i^2}\left[-\cos(\kappa_i b) + \left(Kn\kappa_i + \frac{1}{\kappa_i b}\right)\sin(\kappa_i b)\right]}{\left[\cosh(\kappa_i h) + Kn\kappa_i \sinh(\kappa_i h)\right]\left[\frac{b}{2} + \frac{\sin(2\kappa_i b)}{4\kappa_i}\right]} \cosh(\kappa_i y)\cos(\kappa_i z). \end{aligned} \tag{40}$$

For the numerical solution of the steady, laminar, incompressible and fully developed flow in the microchannel with the rectangular cross-section, the finite difference method is used. The elliptic PDE (17) describing the velocity field is dicretized using the five-point difference formulas of the second order accuracy. The Gauss-Seidel iteration method is applied, which means that in order to evaluate u at grid point i, j, the values of $u_{i-1,j}$, $u_{i,j-1}$ are used from the current iteration and the values of $u_{i+1,j}$, $u_{i,j+1}$ are used from the previous iteration. The finite difference form of (17) used for our numerical computation is therefore

$$u_{i,j}^{n+1} = \frac{1}{\frac{2}{(\Delta b)^2} + \frac{2}{(\Delta h)^2}}\left[\frac{1}{(\Delta b)^2}\left(u_{i+1,j}^{n} + u_{i-1,j}^{n+1}\right) + \frac{1}{(\Delta h)^2}\left(u_{i,j+1}^{n} + u_{i,j-1}^{n+1}\right) - Re\frac{\mathrm{d}p}{\mathrm{d}x}\right], \tag{41}$$

where u is the velocity in the x-direction, n denotes the number of the iteration, $\Delta h = y_{j+1} - y_j$ and $\Delta b = z_{i+1} - z_i$ are the step sizes in the direction of y and z, which are constant in the entire computational domain, and the indices i and j correspond to the position of the actual finite difference cell in the direction of z and y, respectivelly. The velocity slip at microchannel walls, i. e. for $y = h$ and $z = b$, is expresed by the boundary conditions

$$u_{i,py}^{n+1} = \frac{Kn}{\Delta h}\cdot\frac{u_{i,py-1}^{n}}{1 + \frac{Kn}{\Delta h}}, \quad u_{pz,j}^{n+1} = \frac{Kn}{\Delta b}\cdot\frac{u_{pz-1,j}^{n}}{1 + \frac{Kn}{\Delta b}}, \tag{42}$$

where py and pz is the total number of cells in direction of y and z, respectivelly. The symmetry condition for $y = 0$ and $z = 0$ is

$$u_{i,1}^{n+1} = u_{i,2}^{n}, \quad u_{1,j}^{n+1} = u_{2,j}^{n}. \tag{43}$$

The comparison of the results obtained using the analytical and numerical solution is made in the following figures. For the pressure driven flow of argon ($\gamma = 1.67$, $\rho = 1.35\,\mathrm{kg\,m^{-3}}$, $p_1 = 202\,650\,\mathrm{Pa}$, $p_2 = 25\,000\,\mathrm{Pa}$, $\eta = 2.588 \cdot 10^{-5}\,\mathrm{Pa\,s}$) we obtain $Re = 0.015$ and $Kn = 0.032\,6$. The dimensionless sizes of the microchannel are considered as $h = 0.262\,5$, $b = 5.25$ and $L = 2625$. In fig. 2, where the velocity profiles for given y- and z-cuts are shown, our analytical solution is verified using the comparison with the numerical solution. The cuts are considered in the middle of the channel (for $y = 0$ or $z = 0$), in the quarter of the corresponding channel size ($y = h/2$, $z = b/2$) and at the wall ($y = h$, $z = b$). The good agreement of the obtained results indicates the correctness of our analytical formulation. In fig. 3, the velocity profile in the yz plane is shown, illustrating the velocity slip at the microchannel walls caused by the relatively high Knudsen number.

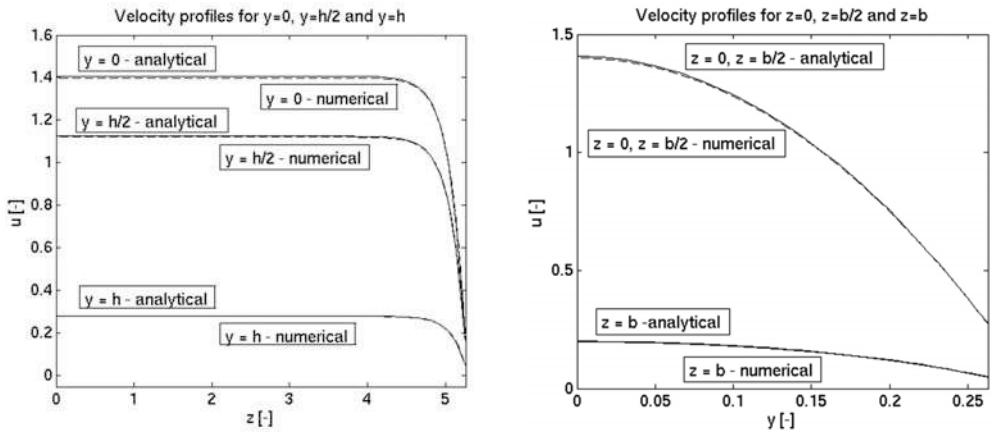

Fig. 2. Numerical and analytical dimensionless velocity profiles for given y- and z-cuts

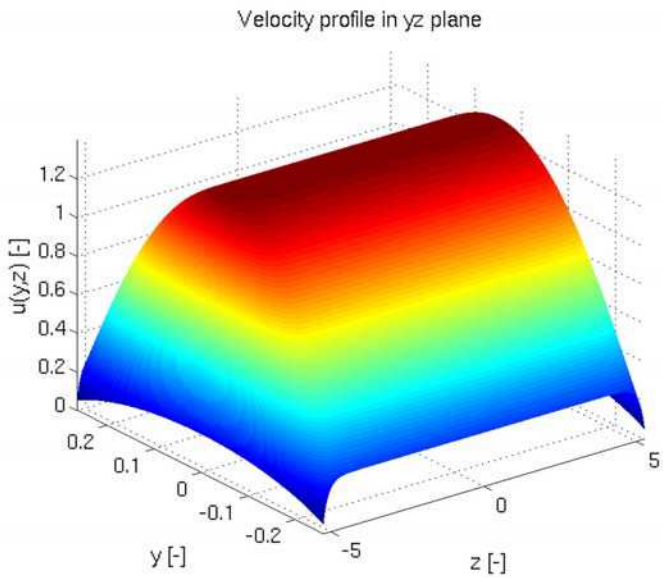

Fig. 3. Dimensionless velocity profile in the yz plane.

4. Analytical and numerical solution of heat transfer

In the case of heat transfer, we will focus on the temperature distribution described by the equation (19) with the boundary conditions (14) and (20). Similarly as in the previous case, we write the general solution as

$$T(y,z) = T^{(1)}(z) + T^{(2)}(y,z). \tag{44}$$

After the substitution of (44) into (19), we get

$$\frac{\mathrm{d}^2 T^{(1)}(z)}{\mathrm{d}z^2} = Pe\frac{\partial T}{\partial x}, \tag{45}$$

$$\frac{\partial^2 T^{(2)}(y,z)}{\partial y^2} + \frac{\partial^2 T^{(2)}(y,z)}{\partial z^2} = 0. \tag{46}$$

The solution of (45) can be expressed as

$$T^{(1)}(z) = \frac{1}{2} Pe \frac{\partial T}{\partial x} z^2 + D_1 z + D_2 \tag{47}$$

and the solution of (46) is considered to be the product of two functions $\varphi(y)$ and $\psi(z)$

$$T^{(2)}(y,z) = \varphi(y)\psi(z). \tag{48}$$

Further, we substitute (48) into (46) which results in two differential equations (analogous to (27)) having the solution

$$\varphi(y) = A_3 e^{\chi y} + A_4 e^{-\chi y} \quad \text{and} \quad \psi(z) = B_3 \cos(\chi z) + B_4 \sin(\chi z), \tag{49}$$

where the constants D_1, D_2, A_3, A_4, B_3, B_4, χ will be determined from the boundary conditions. The general solution of the problem can be written in the form

$$T(y,z) = \frac{1}{2} Pe \frac{\partial T}{\partial x} z^2 + D_1 z + D_2 + \left[A_3 e^{\chi y} + A_4 e^{-\chi y}\right] \left[B_3 \cos(\chi z) + B_4 \sin(\chi z)\right]. \tag{50}$$

If we take into account the symmetry conditions (14), we get $D_1 = B_4 = 0$, $A_3 = A_4$ and this general solution reduces to

$$T(y,z) = \frac{1}{2} Pe \frac{\partial T}{\partial x} z^2 + D_2 + B \cosh(\chi y) \cos(\chi z) \tag{51}$$

where $B = 2A_3 B_3$. In order to determine the constants B, D_2, χ, we use the boundary conditions (20)

$$T_w - \frac{1}{2} Pe \frac{\partial T}{\partial x} z^2 - D_2 - B \cosh(\chi h) \cos(\chi z) = \frac{2\gamma}{\gamma + 1} \frac{Kn}{Pr} \chi B \sinh(\chi h) \cos(\chi z), \tag{52}$$

$$\begin{aligned} T_w - \frac{1}{2} Pe \frac{\partial T}{\partial x} b^2 - D_2 \quad &- \quad B \cosh(\chi y) \cos(\chi b) = \\ &= \quad \frac{2\gamma}{\gamma + 1} \frac{Kn}{Pr} [Pe \frac{\partial T}{\partial x} b - \chi B \cosh(\chi y) \sin(\chi b)]. \end{aligned} \tag{53}$$

Following two equations result from (53)

$$D_2 = T_w - \frac{1}{2} Pe \frac{\partial T}{\partial x} b^2 - \frac{2\gamma}{\gamma + 1} \frac{Kn}{Pr} Pe \frac{\partial T}{\partial x} b, \tag{54}$$

$$\frac{\cot(\chi b)}{\chi b} = \frac{2\gamma}{\gamma + 1} \frac{Kn}{Pr \cdot b}. \tag{55}$$

The transcendent equation (55) has an infinite number of roots $\chi b = \chi_i b$, $i = 1, \ldots, \infty$, therefore the solution can be expressed as

$$\begin{aligned} T(y,z) \quad &= \quad T_w + \frac{1}{2} Pe \frac{\partial T}{\partial x} \left[z^2 - b^2 \left(1 + \frac{4\gamma}{\gamma + 1} \frac{Kn}{Pr \cdot b} \right) \right] + \\ &+ \quad \sum_{i=1}^{\infty} B_i \cosh(\chi_i y) \cos(\chi_i z). \end{aligned} \tag{56}$$

The constants B_i can be determined similarly as the constants A_i for the velocity. We obtain

$$B_i = \frac{\frac{2}{\chi_i^3} Pe \frac{\partial T}{\partial x} \sin(\chi_i b)}{\left[b + \frac{\sin(2\chi_i b)}{2\chi_i}\right] \left[\cosh(\chi_i h) + \frac{2\gamma}{\gamma+1} \frac{Kn}{Pr} \chi_i \sinh(\chi_i h)\right]} \tag{57}$$

and the final form of the temperature distribution results from the substitution of B_i into (56).

The finite difference method is also used for the numerical solution of the temperature distribution. By applying the Gauss-Seidel iterative method on the elliptic PDE (19) describing the temperature field, we get

$$T_{i,j}^{n+1} = \frac{1}{\frac{2}{(\Delta b)^2} + \frac{2}{(\Delta h)^2}} \left[\frac{1}{(\Delta b)^2} \left(T_{i+1,j}^{n} + T_{i-1,j}^{n+1}\right) + \frac{1}{(\Delta h)^2} \left(T_{i,j+1}^{n} + T_{i,j-1}^{n+1}\right) - Pe \frac{\partial T}{\partial x} \right], \tag{58}$$

where $\partial T/\partial x$ is supposed to be constant. The temperature jump at channel walls is expresed as

$$T_{i,py}^{n+1} = \frac{1}{1+c} \left(c \cdot T_{i,py-1} + T_w\right), \quad T_{pz,j}^{n+1} = \frac{1}{1+d} \left(d \cdot T_{pz-1,j} + T_w\right), \tag{59}$$

where

$$c = \frac{2\gamma}{\gamma+1} \cdot \frac{Kn}{Pr \cdot \Delta h}, \quad d = \frac{2\gamma}{\gamma+1} \cdot \frac{Kn}{Pr \cdot \Delta b}. \tag{60}$$

The symmetry condition for $y = 0$ and $z = 0$ gives

$$T_{i,1}^{n+1} = T_{i,2}^{n}, \quad T_{1,j}^{n+1} = T_{2,j}^{n}. \tag{61}$$

Temperature distributions obtained using our analytical and numerical solution are compared in the following figures. The wall temperature needed for the analysis is chosen as $T_w = 350\,\mathrm{K}$ and the thermal conductivity coefficient is considered to be $a = 0.017\,\mathrm{m}^2/\mathrm{s}$. Other parameters of argon and the dimensionless microchannel sizes are the same as for the velocity distribution investigation. In fig. 4, analytical and numerical profiles of the difference of dimensionless temperatures $T - T_w$ in given y- and z-cuts are compared.

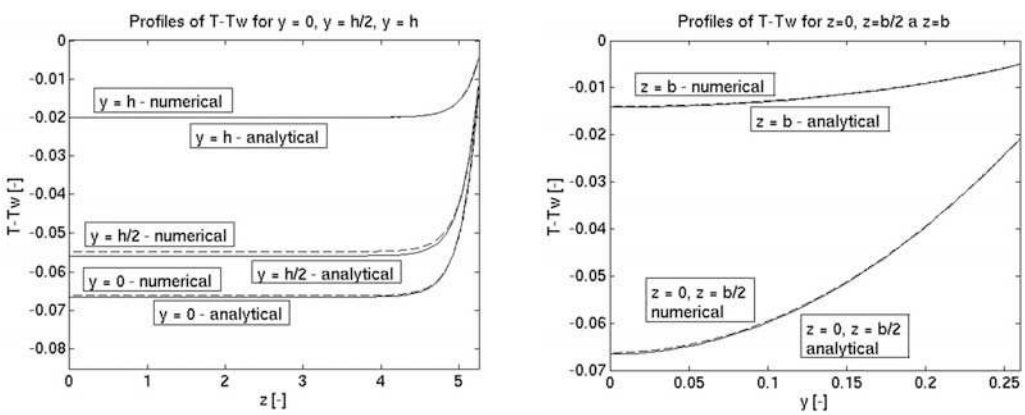

Fig. 4. Numerical and analytical profiles of the difference of dimensionless temperatures $T - T_w$ for given y- and z-cuts

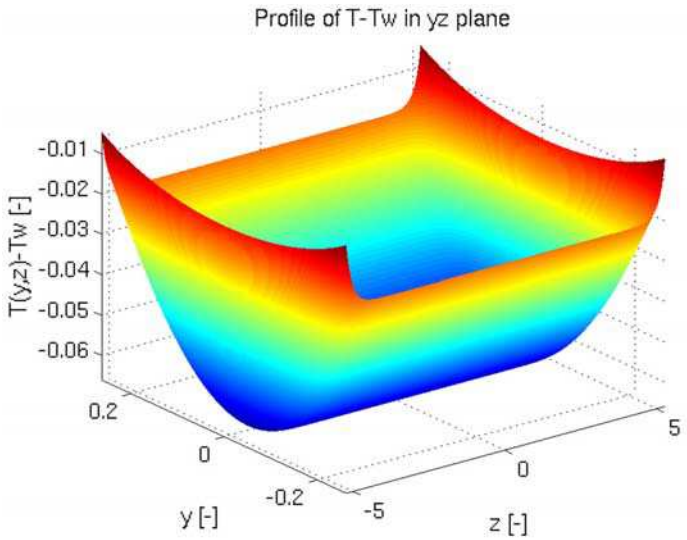

Fig. 5. Profile of the difference of dimensionless temperatures $T - T_w$ in the yz plane

Fig. 5 shows the three-dimensional profile of the difference of dimensionless temperatures $T - T_w$ in the yz plane expressing the temperature jump at the walls as the effect of the slip flow. The good agreement of our analytical and numerical results can be clearly seen in fig. 4, which proves the correctness of our analytical formulation as well as in the case of the velocity field analysis.

5. Conclusion

This study deals with the analytical and numerical solution of gas flow and heat transfer in the microchannel with rectangular cross-section. Our analytical solution is derived using the Fourier method applying the velocity slip and temperature jump boundary conditions that are valid for microflows in the slip flow regime. The good agreement with the numerical solution obtained using the Gauss-Seidel iteration method proves the correctness of our analytical expressions. Moreover, these expressions seems to be simpler for the evaluation then the analytical solution presented in [10]. Our analytical approach can be also applied on the classical steady, laminar, incompressible and fully developed gas flow with non-slip boundary conditions prescribed at the channel walls, which results in

$$\begin{aligned} u(y,z) &= \frac{Re}{2}\frac{\mathrm{d}p}{\mathrm{d}x}\left(z^2-b^2\right) + \\ &+ \sum_{i=1}^{\infty} \frac{16Re\frac{\mathrm{d}p}{\mathrm{d}x}\frac{b^2}{(2i-1)^3\pi^3}(-1^{i-1})}{\cosh\left[\frac{(2i-1)\pi h}{2b}\right]} \cosh\left[\frac{(2i-1)\pi y}{2b}\right] \cos\left[\frac{(2i-1)\pi z}{2b}\right]. \end{aligned}$$

The same expression can be also obtained by setting $Kn = 0$ in (40). Similarly, the temperature distribution for $Kn = 0$ has the form

$$T(y,z) = T_w + \frac{Pe}{2}\frac{\partial T}{\partial x}\left(z^2 - b^2\right) + \\ + \sum_{i=1}^{\infty} \frac{16Pe\frac{\partial T}{\partial x}\frac{b^2}{(2i-1)^3\pi^3}(-1^{i-1})}{\cosh\left[\frac{(2i-1)\pi h}{2b}\right]} \cosh\left[\frac{(2i-1)\pi y}{2b}\right] \cos\left[\frac{(2i-1)\pi z}{2b}\right].$$

In our future study, we want to focus on the analytical and numerical analysis of gas microflow considering the second-order velocity slip and temperature jump boundary conditions at the microchannel walls. Furthermore, we also want to derive the analytical solution of a laminar incompressible slip flow in the inlet part of the rectangular microchannel using the Oseen flow model with the first-order slip flow boundary conditions prescribed at the microchannel walls.

Acknowledgements

This study was supported by the grant GA ČR 101/08/0623 of the Czech Science Foundation.

References

[1] Y. Asako, T. Pi, S. E. Turner, M. Faghri, M., Effect of compressibility on gaseous flows in microchannels, International Journal of Heat and Mass Transfer 46 (2003) 3 041–3 050.

[2] N. Dongari, Ab. Agrawal, Am. Agrawal, Analytical solution of gaseous slip flow in long microchannels, International Journal of Heat and Mass Transfer 50 (2007) 3 411–3 421.

[3] W. A. Ebert, E. M. Sparrow, Slip flow in rectangular and annular ducts, Journal of Basic Engineering 87 (1965) 1 018–1 024.

[4] K. A. Hoffmann, S. T. Chiang, Computational Fluid Dynamics, Engineering Education System, Wichita, USA, 2000.

[5] Ho-E. Jeong, Jae-T. Jeong, Extended Graetz problem including streamwise conduction and viscous dissipation in microchannels, International Journal of Heat and Mass Transfer 49 (2006) 2 151–2 157.

[6] S. G. Kandlikar, S. Garimella, D. Li, S. Colin, M. R. King, Heat transfer and fluid flow in minichannels and microchannels, Elsevier, Amsterdam, 2006.

[7] G. Karniadakis, A. Beskok, N. Aluru, Microflows and Nanoflows: Fundamentals and Simulations, Springer-Verlag, New York, 2005.

[8] E. H. Kennard, Kinetic Theory of Gases, McGraw-Hill Book Company, New York, 1938.

[9] G. L. Morini, Analytical determination of the temperature distribution and Nusselt numbers in rectangular ducts with constant axial heat flux, International Journal of Heat and Mass Transfer 43 (2000) 741–755.

[10] G. L. Morini, M. Spiga, Slip flow in rectangular microtubes, Microscale Thermophysical Engineering 2 (1998) 273–282.

[11] M. Spiga, G. L. Morini, Nusselt numbers in laminar flow for H2 boundary conditions, International Journal of Heat and Mass Transfer 39 (1996) 1 165–1 174.